

# Investigation of orbital momentum profiles of methylpropane (isobutane) by binary ( $e,2e$ ) spectroscopy

J. K. Deng,<sup>a)</sup> G. Q. Li, Y. He, J. D. Huang, H. Deng, X. D. Wang, F. Wang, Y. A. Zhang, C. G. Ning, N. F. Gao, Y. Wang, X. J. Chen, and Y. Zheng<sup>b)</sup>

*Department of Physics, Tsinghua University, Beijing 100084, People's Republic of China*

(Received 2 May 2000; accepted 8 September 2000)

Momentum profiles of the valence orbitals of methylpropane, also known as isobutane ( $\text{CH}_3\text{CH}(\text{CH}_3)\text{CH}_3$ ), have been studied by using a high resolution binary ( $e,2e$ ) electron momentum spectrometer (EMS), at an impact energy of 1200 eV plus the binding energy, and using symmetric noncoplanar kinematics. The coincidence energy resolution of the EMS spectrometer is 0.95 eV full width at half-maximum. The experimental momentum profiles of the valence orbitals are compared with the theoretical momentum distributions calculated using Hartree–Fock (HF) and density functional theory (DFT) methods with the two basis sets of 6-31G and 6-311++G\*\*. The B3LYP functionals are used for the DFT calculations. In general, the experimental momentum distributions are well described by the HF and DFT calculations. The pole strengths of the main ionization peaks from the orbitals in the inner valence are estimated. © 2001 American Institute of Physics. [DOI: 10.1063/1.1321313]

## I. INTRODUCTION

Electron momentum spectroscopy (EMS) has been rapidly developed following the pioneer research of Amaldi *et al.*<sup>1</sup> and Weigold *et al.*<sup>2</sup> It has now become a powerful experimental tool for investigating the electronic structure of atoms, molecules, biomolecules, and condensed matter.<sup>3–8</sup> The technique can access the complete valence shell binding energy range, though with lower energy resolution than in most photoelectron spectroscopy (PES) studies. In particular, EMS measurements of the momentum profiles for individual orbitals in atoms and molecules have been shown to provide a sensitive method for the evaluation and design of accurate self-consistent field as well as highly correlated molecular wave functions and also density functional theory (DFT) methods. The details of EMS experimental techniques and the associated theoretical analysis for atoms, molecules, and condensed matter have been reviewed in detail elsewhere.<sup>3–9</sup>

Up to now, the studies of the electronic structure of small-saturated hydrocarbon molecules have received much interest. This is because not only are these molecules prototypes of larger hydrocarbons, but they are also important species for fuels where reforming of straight chain hydrocarbons into branched chain species is of importance. Saturated hydrocarbon molecules have been widely studied by PES,<sup>10–13</sup> but until recently only the methane and ethane molecules had been studied by EMS,<sup>14–16</sup> due mainly to the limited coincidence energy resolution of binary ( $e,2e$ ) spectrometers, which has been typically 1.2–1.5 eV full width at half-maximum (FWHM) at an impact energy of 1200 eV plus the binding energy. It has only recently become possible to investigate larger hydrocarbon molecules such as

propane<sup>17</sup> and *n*-butane<sup>18</sup> and this has been achieved at Tsinghua University by obtaining a coincidence energy resolution of 0.95 eV FWHM with a multichannel EMS spectrometer.<sup>19</sup>

As part of a series study of saturated hydrocarbon molecules using the high energy resolution EMS spectrometer at Tsinghua University, we now report the measurements of orbital momentum profiles for the complete valence shell of methylpropane ( $\text{CH}_3\text{CH}(\text{CH}_3)\text{CH}_3$ ), also known as isobutane. The experiment was performed at impact energy of 1200 eV plus the binding energy and using symmetric noncoplanar kinematics.<sup>3</sup> The measured results of the binding energy spectra from 8 to 32 eV and the momentum distributions of the highest occupied molecular orbital (HOMO) and NHOMO summed orbitals ( $6a_1+5e$ ) of methylpropane have been recently reported.<sup>20</sup> A sufficiently high impact energy (>1200 eV) and momentum transfer were used to ensure the validity of the plane wave impulse approximation. The relatively large number of electrons in methylpropane renders accurate quantum chemical calculations quite difficult, thus the availability of good EMS experimental data is an important aid for developing satisfactory theoretical descriptions of both binding energies and the valence orbital electron densities in hydrocarbons.

## II. THEORETICAL BACKGROUND

In a binary ( $e,2e$ ) experiment, the scattered and the ionized electrons are detected at the same kinetic energies and the same polar angles in symmetric noncoplanar scattering geometry. Under conditions of high impact energy and high momentum transfer, the target electron essentially undergoes a clean “knock-out” collision and the plane wave impulse approximation (PWIA) provides a very good description of the collision. In the PWIA, the momentum  $p$  of the electron prior to knock-out is related to the azimuthal angle by<sup>1</sup>

<sup>a)</sup>Electronic mail: djkdmp@mail.tsinghua.edu.cn

<sup>b)</sup>Also at: Department of Chemistry, University of British Columbia, 2036 Main Mall, Vancouver, British Columbia V6T 1Z1, Canada.

$$p = [(2p_1 \cos \theta_1 - p_0)^2 + (2p_1 \sin \theta_1 \sin(\phi/2))^2]^{1/2}, \quad (1)$$

where  $p_1 = p_2 = \sqrt{2E_1}$  is the magnitude of the momentum of each outgoing electron and  $p_0 = \sqrt{2E_0}$  is the momentum of the incident electron (both in atomic units). Under these conditions the kinematic factors are effectively constant,<sup>3</sup> the EMS cross section for randomly oriented gas-phase targets,  $\sigma_{\text{EMS}}$ , can be given by

$$\sigma_{\text{EMS}} \propto S_f^2 \int d\Omega |\langle \mathbf{p} \Psi_f^{N-1} | \Psi_i^N \rangle|^2, \quad (2)$$

where  $\mathbf{p}$  is the momentum of the target electron prior to ionization and  $S_f^2$  is pole strength and defined in Ref. 21.  $|\Psi_f^{N-1}\rangle$  and  $|\Psi_i^N\rangle$  are the total electronic wave functions for the final ion state and the target molecule ground (initial) state, respectively. The  $\int d\Omega$  represents the spherical average due to the randomly oriented gas phase target. The overlap of the ion and neutral wave functions in Eq. (2) is known as the Dyson orbital while the square of this quantity is referred to as an ion-neutral overlap distribution (OVD). Thus, the  $(e,2e)$  cross section is essentially proportional to the spherical average of the square of the Dyson orbital in momentum space.

Equation (2) is greatly simplified by using the target Hartree–Fock approximation (THFA). Within the THFA, only final (ion) state correlation is allowed and the many-body wave functions  $|\Psi_f^{N-1}\rangle$  and  $|\Psi_i^N\rangle$  are approximated as independent particle determinants of ground state target Hartree–Fock orbitals. In this approximation Eq. (2) reduces to

$$\sigma_{\text{EMS}} \propto S_j^f \int d\Omega |\psi_j(p)|^2, \quad (3)$$

where  $\psi_j(p)$  is the one-electron momentum space canonical Hartree–Fock orbital wave function for the  $j$ th electron, corresponding to the orbital from which the electron was ionized,  $S_j^f$  is the spectroscopic factor, the probability of the ionization event producing a one-hole configuration of the final ion state. The integral in Eq. (3) is known as the spherically averaged one-electron momentum distribution. To this extent EMS has the ability to image the electron density in individual “orbitals” selected according to their binding energies.

Equation (2) has recently been reinterpreted<sup>22</sup> in the context of Kohn–Sham DFT and the target Kohn–Sham Approximation (TKSA) gives a result similar to Eq. (3) but with the canonical Hartree–Fock orbital replaced by a momentum space Kohn–Sham orbital  $\psi_j^{\text{KS}}(p)$ ,

$$\sigma_{\text{EMS}} \propto \int d\Omega |\psi_j^{\text{KS}}(\mathbf{p})|^2. \quad (4)$$

It should be noted that an accounting of electron correlation effects in the target ground state is included in the TKSA via the exchange correlation potential. A more detailed description of the TKSA-DFT method may be found elsewhere.<sup>22</sup>

In the present work, the Hartree–Fock calculations of the momentum profiles were performed by using Eq. (3)

with two basis sets of 6-31G and 6-311++G\*\*. The DFT calculations were carried out using the GAUSSIAN94 program with the B3LYP functionals<sup>23–25</sup> and the two basis sets for the Hartree–Fock (HF) calculations.

The 6-31G basis of Pople and the co-workers<sup>26</sup> is a split-valence basis comprised of an inner valence shell of six  $s$ -type Gaussians and an outer valence shell that has been split into two parts represented by three and one primitives, respectively. Thus carbon atoms have a  $(10s,4p)/[3s,2p]$  contraction and hydrogen atoms have a  $(4s)/[2s]$  contraction. A total of 56 CGTO is for methylpropane.

The 6-311++G\*\* is an augmented version by Pople *et al.* The outer valence shell is split into three parts and represented by three, one, and one primitives. Very diffused  $s$  and  $p$  functions, and spherical  $d$ -type polarization functions are added for carbon atoms, and a diffused  $sp$  shell and  $p$ -type polarization functions are added hydrogen atoms.<sup>26–28</sup> Thus a  $(12s,6p,1d)$  contracts to  $[5s,4p,1d]$  for C, and a  $(6s,1p)$  to  $[4s,1p]$  for H. The number of CGTO is 158 for methylpropane.

The optimized geometry of methylpropane has been used for all the calculations. In order to compare the calculated cross-sections with the experimental electron momentum profiles the effects of the finite spectrometer acceptance angles in both  $\theta$  and  $\phi$  ( $\Delta\theta = \pm 0.6^\circ$  and  $\Delta\phi = \pm 1.2^\circ$ ) were included using the Gaussian-weighted planar grid method.<sup>29</sup>

### III. EXPERIMENTAL METHODS

An energy-dispersive multichannel electron momentum spectrometer with a symmetric noncoplanar geometry is used in the experiment of this work. The details of the spectrometer constructed at Tsinghua University have been reported previously.<sup>19</sup> An electron beam, produced from a LaB<sub>6</sub> filament of the vertically mounted electron gun, is accelerated and focused into the interaction region through a series of electron optical lenses and beam deflection systems. Two hemispherical electron energy analyzers, mounted on two independent horizontal concentric turntables, each having a five-element cylindrical retarding lens system, are used for energetically selecting the scattered and ejected electrons in the experiment. In the present work, the polar angles of both analyzers are kept fixed at  $45^\circ$ . One analyzer turntable is kept in a fixed position while the other is rotated by a computer controlled stepping motor to vary the relative azimuthal angle  $\phi$  over a range of  $\pm 30^\circ$ . The electrons are linearly dispersed by each hemispherical analyzer along the radius direction at the exit focal plane according to their input energies. Each energy analyzer has a position sensitive detector consisting of two microchannel plates in a double chevron configuration and a resistive anode. All components of the spectrometer are placed in a mu-metal shielded vacuum system. A typical base pressure of the system is on the order of  $10^{-7}$  Torr.

The associated electronics and software of the spectrometer were used for data acquisition, fast timing logic, operation control such as the incident energy and the movable detector rotation, and computer interfacing. The fast timing pulses coupled from the back of the resistive anode of each

detector are amplified, discriminated, and fed to a time-to-amplitude converter to produce a coincidence time spectrum. True and random coincidences are then separated by two single channel analyzers (SCAs) set in appropriate windows. The slow energy (position) signals from resistive anode of each detector are amplified and digitized by a home-built multichannel analog-to-digital converter. The accumulated energy signals are then selected by output pulses from the SCAs to determine coincidence and random background. A true coincidence energy spectrum is derived by subtraction of the random background from the coincidence position spectrum.

In the present experiment, the pass energy of each analyzer was set at 50 eV with an energy range of 8.0 eV ( $600 \pm 4$  eV) covered by each detector. Electron impact ionization was carried out at impact energy of 1200 eV plus the binding energy under the symmetric noncoplanar geometry. The summed energy range is then from 1192 to 1208 eV for the two outgoing electrons. The energy resolution obtained in a coincidence experiment is the convolution of the two analyzer response functions and the energy spread of the incident electron beam. The energy resolution depends on the deceleration ratio of the retarding lens system. The coincidence energy resolution of the spectrometer was measured to be 0.95 eV FWHM from the experiment on the helium 1s state. The experimental momentum resolution is estimated to be about 0.1 a.u. from a consideration of the argon 3p angular correlation. The sample of methylpropane from Matheson

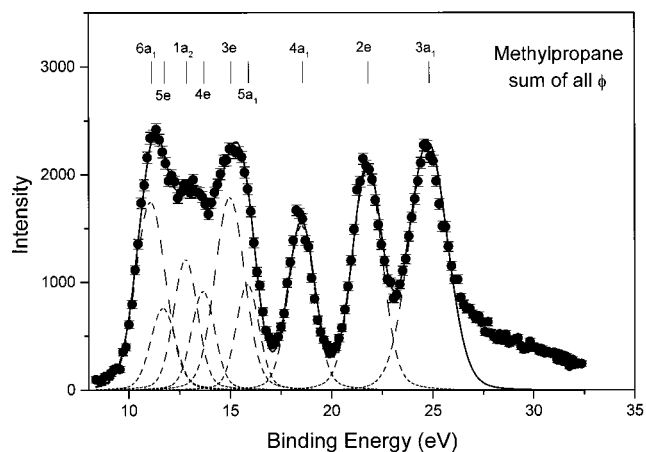


FIG. 1. Valence shell binding energy spectra at an impact energy of 1200 eV plus the binding energy (8–32 eV) for methylpropane at sum of all  $\phi$  angles. The dashed lines represent the fitted Gaussians for individual peaks and the solid line for their sum, i.e., the overall fitted spectra, respectively.

(99.9% purity) was used without further purification. No evidence of impurities was found in the binding energy spectra.

#### IV. RESULTS AND DISCUSSIONS

The point group symmetry of methylpropane is  $C_{3v}$ . According to molecular orbital theory, the ground state electronic configuration can be written as

$$(1a_1)^2(1e)^4(2a_1)^2(3a_1)^2(2e)^4(4a_1)^2(5a_1)^2(3e)^4(4e)^4(1a_2)^2(5e)^4(6a_1)^2.$$

inner-valence
outer-valence

In the ground state, the 34 electrons are arranged in 17 doubly occupied orbitals in the independent particle description. The valence electrons in methylpropane are distributed in 13 molecular orbitals and 4 of the orbitals are degenerate. All the canonical molecular orbitals are either  $a$  type or  $e$  type. The four  $e$ -type orbitals are each double degenerate. The assignment of the order of occupation for these valence orbitals, both by PES experiments and by molecular orbital calculations, has been discussed in detail in Refs. 10–13.

To obtain the experimental momentum profiles, 11 binding energy spectra over the energy range of 8–32 eV were collected at the out-of-plane azimuthal angles  $\phi = 0^\circ, 2^\circ, 4^\circ, 6^\circ, 8^\circ, 10^\circ, 12^\circ, 14^\circ, 16^\circ, 20^\circ,$  and  $24^\circ$  in a series of sequential repetitive scans. Figure 1 shows the valence shell binding energy spectra of methylpropane in the range of 8–32 eV summed over all the  $\phi$  angles at the impact energy of 1200 eV plus the binding energy. The spectra in Fig. 1 were fitted with a set of individual Gaussian peaks whose widths are combinations of the EMS instrumental energy resolution and the corresponding Franck–Condon widths derived from high resolution PES data.<sup>7</sup> The fitted Gaussians for individual peaks are indicated by dashed lines while their sum, i.e., the overall fitted spectra, are represented by the solid lines. The

relative energy values are given by the relative ionization energies determined by high resolution PES.

The PES spectra of the six orbitals of the outer valence region have been reported by Kimura *et al.*<sup>10</sup> using a He I radiation source. In this work,<sup>10</sup> the vertical ionization potentials of the  $6a_1, 5e, 1a_2, 4e, 3e,$  and  $5a_1$  orbitals were determined to be 11.13, 11.7 (12.1), 12.85, 13.52 (13.9), 14.86 (15.3), and 15.95 eV, respectively. Since methylpropane is a nonlinear molecule, the PES spectra are complicated by the Jahn–Teller effect. The energy splitting positions, due to the Jahn–Teller effect, of the degenerate  $5e, 4e,$  and  $3e$  orbitals are indicated in the corresponding brackets (see the previous text). These PES studies were extended by Potts *et al.*<sup>13</sup> using a He II radiation source which also covered some of the inner valence region of methylpropane and structures at 18.37, 21.9, and 24.8 eV were assigned to the  $4a_1, 2e,$  and  $3a_1$  orbitals, respectively.

In the present EMS measurements, average vertical ionization potentials of the  $6a_1, 5e, 1a_2, 4e, 3e,$  and  $5a_1$  outer orbitals are determined to be 11.13, 11.75, 12.85, 13.71, 15.03, and 15.91 eV, and the three inner orbitals of the  $4a_1, 2e,$  and  $3a_1$  are 18.58, 21.83, and 24.83 eV, respectively. The measured EMS binding energies shown in

TABLE I. Ionization energy for methylpropane (eV).

Orbital	Experimental results				Theoretical orbital energies of HF/6-311++G** <sup>a</sup>
	EMS <sup>a</sup>	PES <sup>b</sup>	PES <sup>c</sup>	PES <sup>d</sup>	
6a <sub>1</sub>	11.13	11.13		11.4	12.46
5e	11.75	11.7(12.1)		12.1	12.58
1a <sub>2</sub>	12.85	12.85		12.8	13.77
4e	13.71	13.52(13.9)		13.4	14.45
3e	15.03	14.86(15.3)		14.9	16.05
5a <sub>1</sub>	15.91	15.95		16.0	17.16
4a <sub>1</sub>	18.58		18.37		20.77
2e	21.83		21.9		25.18
3a <sub>1</sub>	24.83		24.81		29.48

<sup>a</sup>This work.<sup>b</sup>From Ref. 10.<sup>c</sup>From Ref. 13.<sup>d</sup>From Ref. 12.

Fig. 1 are consistent with the PES values<sup>12,13</sup> for the outer and inner valence orbitals. A comparison of the valence shell binding energies of methylpropane of this work and the experimental PES data<sup>10–13</sup> and the Hartree–Fock values is given in Table I. It can be seen that the present measured EMS data are consistent with the previously published high resolution PES data and also the calculations. In addition, some rather weak structure due mainly to correlation effects in the target or in the residual ion final states is also observed above 26 eV.

Experimental momentum profiles (XMPs) have been extracted by deconvolution of the sequentially obtained angular-correlated binding energy spectra, and therefore the relative normalization for the different transitions are maintained. For all the orbitals, the various theoretical momentum profiles (TMPs) are obtained with the methods described in Sec. II and the experimental instrumental angular resolutions have been incorporated in the calculations using the UBC RESFOLD program based on the GW-PG method.<sup>29</sup> Experimental data and theoretical values have been placed on a common intensity scale by normalizing the summed experimental to the DFT-B3LYP/6-311++G\*\* theoretical momentum profiles for the 6a<sub>1</sub>+5e orbitals (see Fig. 2) and the relative normalization is preserved for other orbitals.

The six outer-valence orbitals, 6a<sub>1</sub>, 5e, 1a<sub>2</sub>, 4e, 3e, and 5a<sub>1</sub>, are not well separated experimentally due to their small energy separations although individual Gaussian peaks were fitted into the binding energy spectrum of Fig. 1. Therefore, summed momentum distributions of the 6a<sub>1</sub>+5e, 1a<sub>2</sub>+4e, and 3e+5a<sub>1</sub> orbitals are, respectively, discussed for comparison between experiment and theory.

The first peak and the second peak, positioned at 11.13 and 11.75 eV, respectively, in the EMS binding energy spectrum in Fig. 1, are due to the 6a<sub>1</sub> and 5e orbitals, i.e., HOMO and NHOMO. Figure 2 shows that the summed XMPs have a double-peak distribution peaked at ~0.25 and ~1.2 a.u., respectively. The intensity of the first peak is greater than the second one in the momentum distribution. According to the HF and DFT-B3LYP calculations, the 6a<sub>1</sub> orbital has an “s-p type” distribution while the 5e orbital has a “p-p type” distribution, as shown under the summed

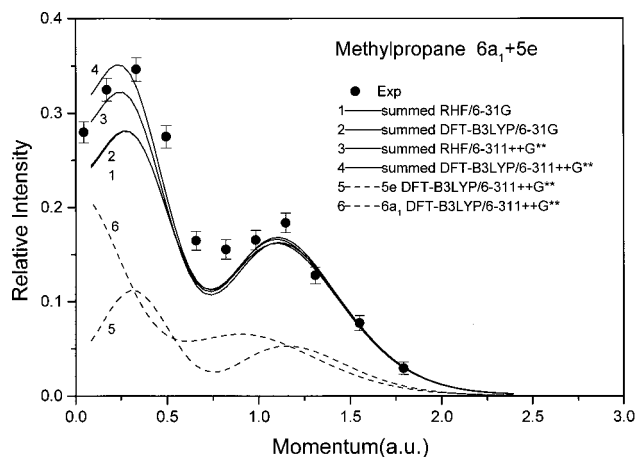


FIG. 2. Experimental and calculated spherically averaged momentum distributions for the summed and individual orbitals of the 6a<sub>1</sub> and 5e orbitals of methylpropane. The summed TMPs are calculated by using Hartree–Fock (curves 1 and 3) and DFT-B3LYP (curves 2 and 4) methods with the 6-31G and 6-311++G\*\* basis sets. The TMPs of individual orbitals are calculated by using the DFT-B3LYP method with the 6-311++G\*\* basis set (curves 5 and 6).

momentum distribution curves in Fig. 2. The summed theoretical momentum distribution of these two orbitals therefore has a double-peak distribution, consistent with the XMPs. The comparison of the summed XMPs with various calculations in Fig. 2 shows that the four TMPs reproduce the experimental data reasonably well, particularly in the momentum range above 0.5 a.u., and the two lower level calculations (curves 1 and 2) with the 6-31G basis set underestimate experimental intensity in the low momentum range from 0.0 to 0.5 a.u. The result of DFT-B3LYP with 6-311++G\*\* provides the best fit to the XMPs.

The momentum distributions of the 1a<sub>2</sub> and 4e orbitals, peaked at 12.85 and 13.71 eV in Fig. 1, are summed and they have “p-type” momentum distributions as indicated by the DFT-B3LYP calculations (curves 5 and 6) in Fig. 3. The four summed TMPs are very similar and fit to the summed XMPs very well in the momentum region above 0.5 a.u. However, there is a significant discrepancy between theoretical calculation and experimental data below the momentum of 0.5 a.u. and the TMPs underestimate the experimental intensity. The discrepancy between experiment and theory in the low momentum region is probably due to inaccuracies in the Gaussian fitting procedures since the nearby two ionization peaks, i.e., the first peak and the second peak in the binding energy spectra in Fig. 1, are very close, and some intensity of the 6a<sub>1</sub>+5e peak could leak into the 1a<sub>2</sub>+4e peak in the low momentum range (see XMPs in Figs. 2 and 3). Another possible source for the discrepancy in the low momentum range could be because of the distorted wave effects since the 4e orbital of methylpropane is a π\*-like molecular orbital. It has been found<sup>30–32</sup> that such orbitals usually produce a “turn-up” of the cross section in the low momentum range, and this behavior is similar to the low-p effect observed in atomic d-orbital XMPs. This situation is also probably the case for the 4e orbital of methylpropane. Such effects in atoms have been attributed to distorted wave effects that increase the calculated cross sections at low p as

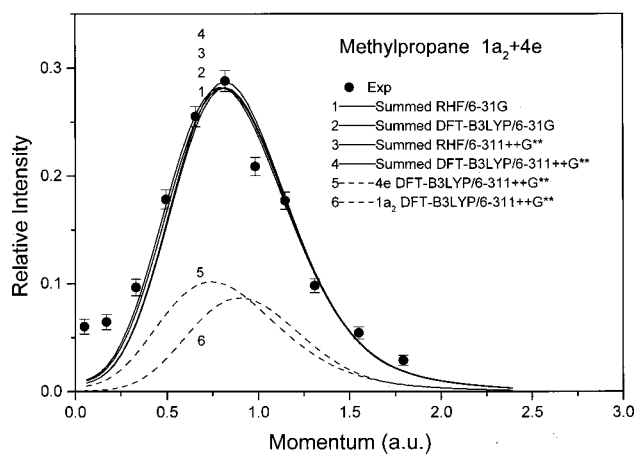


FIG. 3. Experimental and calculated spherically averaged momentum distributions for the summed and individual orbitals of the  $1a_2$  and  $4e$  orbitals of methylpropane. The summed TMPs are calculated by using Hartree–Fock (curves 1 and 3) and DFT-B3LYP (curves 2 and 4) methods with the 6-31G and 6-311++G\*\* basis sets. The TMPs of individual orbitals are calculated by using the DFT-B3LYP method with the 6-311++G\*\* basis set (curves 5 and 6).

observed in the experimental measurements.<sup>30</sup> Similar behavior has been seen in the XMPs of transition-metal hexacarbonyl HOMOs that are known to be largely metal  $nd$  in character.<sup>33</sup> The corresponding transition-metal atoms show such behavior and this is found to decrease with increase in impact energy<sup>33</sup> in the distorted wave impulse approximation (DWIA) calculations. Unfortunately at present DWIA calculations are possible only for atoms but not for molecules due to the multicenter nature of the latter.

The fifth and sixth ionization peaks at 15.03 and 15.91 eV in the binding energy spectrum in Fig. 1 contain contributions from the  $3e$  and  $5a_1$  orbitals. The  $3e$  orbital has a “ $p$ -type” character while the  $5a_1$  orbital shows an “ $s$ -type” distribution, as indicated in Fig. 4. The summed momentum profile is therefore a mixed “ $s$ - $p$ ” type distribution. It can be seen from the comparison in Fig. 4 that the summed TMPs well reproduce the XMP except for the two lower level calculations (curves 1 and 2) in the low momentum region. A better fit to the XMP by the higher level DFT calculation with 6-311++G\*\* (curve 4) indicates that electron correlation effects are very important for momentum profiles in the low momentum region for the  $3e$  and  $5a_1$  orbitals since the DFT-B3LYP method includes electron correlation effects in the target ground state through the exchange correlation potential.<sup>22</sup>

Unlike these outer valence orbitals, the three inner  $4a_1$ ,  $2e$ , and  $3a_1$  orbitals are clearly separated in the EMS binding energy spectrum (see Fig. 1). The first inner-valence orbital is the  $4a_1$  orbital peaked at 18.58 eV in energy spectrum. Figure 5 shows a comparison between the experimental data and the theoretical calculations, which indicates this orbital has mixed “ $s$ - $p$  type” momentum distributions. It can be seen that all the four calculations using the HF and DFT methods well reproduce the XMP in high momentum region above 0.5 a.u., but the calculations, in particular the two with the 6-311++G\*\* basis set, slightly

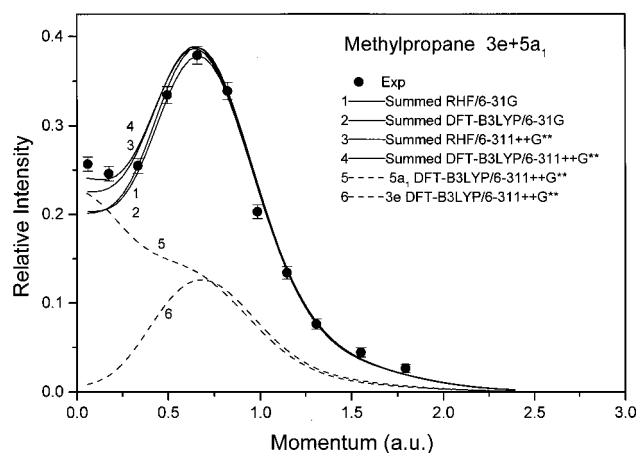


FIG. 4. Experimental and calculated spherically averaged momentum distributions for the summed and individual orbitals of the  $3e$  and  $5a_1$  orbitals of methylpropane. The summed TMPs are calculated by using Hartree–Fock (curves 1 and 3) and DFT-B3LYP (curves 2 and 4) methods with the 6-31G and 6-311++G\*\* basis sets. The TMPs of individual orbitals are calculated by using the DFT-B3LYP method with the 6-311++G\*\* basis set (curves 5 and 6).

overestimate the observed intensity in the low momentum range near the zero momentum.

The next inner-valence orbital is  $2e$  located at 21.83 eV of the EMS binding energy spectrum in Fig. 1. The orbital has a “ $p$ -type” momentum distribution character shown in Fig. 6. The comparison between the experimental data and theoretical calculations in Fig. 6 shows that all four calculations significantly overestimate the experimental intensity. This indicates that some of the transition intensity from this orbital is located in the higher binding energy range due to the final state electron correlation effects. In order to compare the shape of the momentum distribution the DFT-B3LYP/6-311++G\*\* calculation is multiplied by an estimated pole strength of 0.76 and the reproduced momentum profile is represented by curve 5 in Fig. 6. A very good

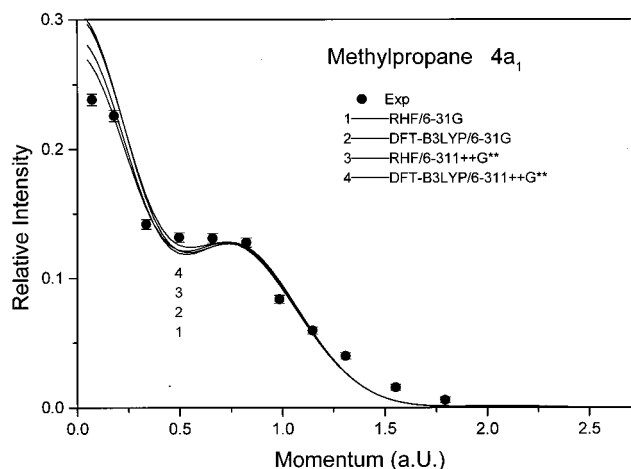


FIG. 5. The experimental and calculated momentum distributions for the inner-valence orbital  $4a_1$  of methylpropane. The TMPs are calculated by using Hartree–Fock (curves 1 and 3) and DFT-B3LYP (curves 2 and 4) methods with the 6-31G and 6-311++G\*\* basis sets.

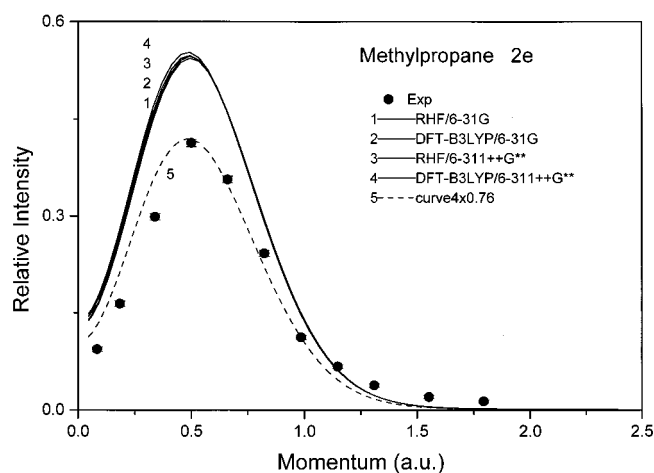


FIG. 6. The experimental and calculated momentum distributions for the inner-valence orbital  $2e$  of methylpropane. The TMPs are calculated by using Hartree–Fock (curves 1 and 3) and DFT-B3LYP (curves 2 and 4) methods with the 6-31G and 6-311++G\*\* basis sets. The curve 5 is due to the curve 4 multiplied by an estimated pole strength of 0.76.

shape agreement between experiment and theory is then achieved.

The last peak, located at 24.83 eV, in the inner valence region of the EMS binding energy spectrum in Fig. 1 is mainly due to the ionization of the  $3a_1$  orbital which has an “s-type” symmetry, as shown in Fig. 7. The calculated momentum distributions for the  $3a_1$  orbital are compared with the experimental data in Fig. 7. It is obvious that all four calculations overestimate the experimental intensity. A strong splitting for the  $3a_1$  orbital into the higher binding energy region is observed (see Fig. 1) due to the final state electron correlation effects. From the above-mentioned discussion about the  $2e$  orbital it should also be noted that this energy range around 24 eV may include some intensity from the  $2e$  orbital. Therefore, estimated spectroscopic factors of

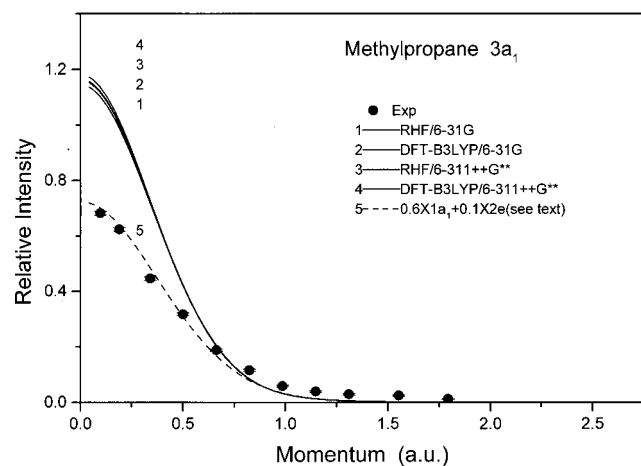


FIG. 7. The experimental and calculated momentum distributions for the inner-valence orbital  $3a_1$  of methylpropane. The TMPs are calculated by using Hartree–Fock (curves 1 and 3) and DFT-B3LYP (curves 2 and 4) methods with the 6-31G and 6-311++G\*\* basis sets. Curve 5 represents a sum of  $0.6 \times$  curve 4 of the  $3a_1$  orbital plus  $0.1 \times$  curve 4 of the  $2e$  orbital in Fig. 6 (see the text).

0.6 and 0.1 are used to multiply the DFT-B3LYP/6-311++G\*\* calculations for the  $3a_1$  and  $2e$  orbitals, respectively, and the summed theoretical curve, represented by curve 5 in Fig. 7, is then compared with the XMP. With the above shape matching scaling factors it can be seen in Fig. 7 that a good fit to experimental data is obtained.

## V. SUMMARY

In summary, the first measurements of the complete valence shell binding energy spectra and the momentum distributions of methylpropane by the electron momentum spectroscopy are reported. The experimental momentum distributions are compared with the associated calculations. The binding energies are in excellent agreement with previously published PES data. The experimental momentum profiles are well described by Hartree–Fock 6-311++G\*\* calculations. The DFT calculations using B3LYP functionals with the 6-311++G\*\* basis set also give a good agreement with the experiments.

## ACKNOWLEDGMENTS

We are grateful to the National Natural Science Foundation of China (NSFC) for financial support of this work. The authors would also like to acknowledge the help of Professor Zhu Qihe.

- <sup>1</sup>U. Amaldi, A. Egidi, R. Marconero, and G. Pizzella, *Rev. Sci. Instrum.* **40**, 1001 (1969).
- <sup>2</sup>E. Weigold, S. T. Hood, and O. J. O. Teubner, *Phys. Rev. Lett.* **20**, 475 (1973).
- <sup>3</sup>I. E. McCarthy and E. Weigold, *Rep. Prog. Phys.* **91**, 789 (1991), and references therein.
- <sup>4</sup>C. E. Brion, *Phys. Elec. At. Coll.*, edited by T. Andersen (AIP Press, New York, 1993), p. 350, and references therein.
- <sup>5</sup>K. T. Leung, *Sci. Prog.* **75**, 157 (1991).
- <sup>6</sup>M. A. Coplan, J. H. Moore, and J. P. Doering, *Rev. Mod. Phys.* **66**, 985 (1994).
- <sup>7</sup>Y. Zheng, J. J. Neville, and C. E. Brion, *Science* **270**, 786 (1995); *J. Am. Chem. Soc.* **118**, 10533 (1996).
- <sup>8</sup>M. Vos and I. E. McCarthy, *Rev. Mod. Phys.* **67**, 713 (1995).
- <sup>9</sup>I. E. McCarthy, *Aust. J. Phys.* **51**, 593 (1998).
- <sup>10</sup>K. Kimura, S. Katsumata, Y. Achiba, T. Yamazaki, and S. Iwata, *Handbook of HeI Photoelectron Spectra of Fundamental Organic Molecules* (Japan Scientific Society, Tokyo, 1981).
- <sup>11</sup>G. Bieri and L. Asbrink, *J. Electron Spectrosc. Relat. Phenom.* **20**, 149 (1980).
- <sup>12</sup>J. N. Murrell and W. Schmidt, *J. Chem. Soc., Faraday Trans. 2* **68**, 1709 (1972).
- <sup>13</sup>A. W. Potts and D. Streets, *J. Chem. Soc., Faraday Trans. 2* **70**, 875 (1974).
- <sup>14</sup>S. T. Hood, E. Weigold, I. E. McCarthy, and P. J. O. Teubner, *Nature (London)* **245**, 65 (1973).
- <sup>15</sup>S. Dey, A. J. Dixon, I. E. McCarthy, and E. Weigold, *J. Electron Spectrosc. Relat. Phenom.* **9**, 397 (1976).
- <sup>16</sup>S. A. C. Clark, T. J. Reddish, C. E. Brion, E. R. Davidson, and R. Frey, *Chem. Phys.* **143**, 1 (1990).
- <sup>17</sup>W. N. Pang, R. C. Shang, N. F. Gao, W. X. Zhang, X. J. Chen, Y. Zheng, and C. E. Brion, *Chem. Phys. Lett.* **299**, 207 (1999).
- <sup>18</sup>W. N. Pang, R. C. Shang, N. F. Gao, W. X. Zhang, J. F. Gao, J. K. Deng, X. J. Chen, and Y. Zheng, *Phys. Lett. A* **248**, 230 (1998).
- <sup>19</sup>Y. Zheng, W. N. Pang, R. C. Shang, X. J. Chen, C. E. Brion, T. K. Ghanty, and E. R. Davidson, *J. Chem. Phys.* **111**, 9526 (1999).
- <sup>20</sup>J. K. Deng *et al.*, *Chem. Phys. Lett.* **313**, 134 (1999).
- <sup>21</sup>Y. Zheng, C. E. Brion, M. J. Brunger, K. Zhao, A. M. Grisogono, S.

- Braidwood, E. Weigold, S. J. Chakravorty, E. R. Davidson, A. Sgamellotti, and W. Von Niessen, *Chem. Phys.* **212**, 269 (1996).
- <sup>22</sup>P. Duffy, D. P. Chong, M. E. Casida, and D. R. Salahub, *Phys. Rev. A* **50**, 4707 (1994).
- <sup>23</sup>C. Lee, W. Yang, and R. G. Parr, *Phys. Rev. B* **37**, 785 (1988).
- <sup>24</sup>B. Miehlich, A. Savin, H. Stoll, and H. Preuss, *Chem. Phys. Lett.* **157**, 200 (1989).
- <sup>25</sup>A. D. Becke, *J. Chem. Phys.* **98**, 5648 (1996).
- <sup>26</sup>R. Krishnan, M. J. Frisch, and J. A. Pople, *J. Chem. Phys.* **72**, 4244 (1980).
- <sup>27</sup>T. Clark, J. Chandrasekhar, G. W. Spitznagel, and P. V. R. Schleyer, *J. Comput. Chem.* **4**, 294 (1983).
- <sup>28</sup>M. J. Frisch, J. A. Pople, and J. S. Binkley, *J. Chem. Phys.* **80**, 3265 (1984).
- <sup>29</sup>P. Duffy, M. E. Casida, C. E. Brion, and D. P. Chong, *Chem. Phys.* **159**, 347 (1992).
- <sup>30</sup>C. E. Brion, Y. Zheng, J. Rokle, J. J. Neville, I. E. McCarthy, and J. Wang, *J. Phys. B* **31**, L223 (1998).
- <sup>31</sup>J. Rolke, Y. Zheng, C. E. Brion, Z. Shi, S. Wolfe, and E. R. Davidson, *Chem. Phys.* **244**, 1 (1999).
- <sup>32</sup>C. E. Brion and Y. Zheng (unpublished).
- <sup>33</sup>J. Rolke, Y. Zheng, C. E. Brion, S. J. Chakravorty, E. R. Davidson, and I. E. McCarthy, *Chem. Phys.* **215**, 191 (1997).